DØ Note 5443-CONF

Search for $t\bar{t}$ Resonance in the Lepton+Jets Final State in $p\bar{p}$ Collisions at $\sqrt{s} = 1.96\,\text{TeV}$

The DØ Collaboration
URL http://www-d0.fnal.gov
(Dated: July 20, 2007)

A search for a narrow-width heavy resonance decaying into top quark pairs ($X \to t\bar{t}$) in $p\bar{p}$ collisions at $\sqrt{s} = 1.96\,\text{TeV}$ has been performed using data collected with the DØ detector at the Fermilab Tevatron collider. This analysis considers $t\bar{t}$ candidate events in the lepton+jets channel using a neural network tagger to identify b-jets and the $t\bar{t}$ invariant mass distribution to search for evidence of resonant production. The analyzed dataset corresponds to an integrated lumiosity of approximately $0.9\,\text{fb}^{-1}$. We find no evidence for a narrow resonance X decaying to $t\bar{t}$. Therefore we set upper limits on $\sigma_X \times B(X \to t\bar{t})$ for different hypothesized resonance masses using a Bayesian approach. Within a topcolor-assisted technicolor model, the existence of a leptophobic Z' boson with mass $M_{Z'} < 680\,\text{GeV}$ and width $\Gamma_{Z'} = 0.012 M_{Z'}$ can be excluded at 95% C.L..

Preliminary Result for Summer 2007 Conferences

I. INTRODUCTION

The top quark has by far the largest mass of all the known fermions. Heavy, yet unknown resonances may play a role in the production of top pairs and add a resonant part to the Standard Model mechanism. Such resonant production are suggested for massive Z-like bosons in extended gauge theories [1], Kaluza Klein states of the gluon or Z [2, 3], axigluons [4], topcolor [5], and other beyond the Standard Model theories. Independent of the exact model a resonant production mechnism should be visible in the $t\bar{t}$ invariant mass distribution.

In this analysis a model-independent search for a narrow-width heavy resonance X decaying into $t\bar{t}$ is performed. In the framework of the SM, the top quark decays into a W boson and b quark nearly 100% of the time. The $t\bar{t}$ event signature is fully determined by the W boson decay modes. In this analysis, we consider only the lepton+jets (ℓ+jets, where $\ell = e$ or μ) final state, which results from the leptonic decay of one of the W bosons and the hadronic decay of the other. The event signature is one isolated electron or muon with high transverse momentum (p_T), large transverse energy imbalance ($\not\!\!E_T$) due to the undetected neutrino, and at least four jets, two of which result from the hadronization of b quarks.

The analyzed dataset corresponds to an integrated luminosity of $913\,\mathrm{pb}^{-1}$ in the e+jets channel and $871\,\mathrm{pb}^{-1}$ in the μ+jets channel, collected between August 2002 and December 2005. The signal-to-background ratio is improved by identifying b-jets using a neural network based b-tagging algorithm. After b-tagging, the dominant physics background for a resonance signal is non-resonant SM $t\bar{t}$ production. Smaller contributions arise from the direct production of W bosons in association with four or more jets (W+jets), as well as instrumental background originating from multijet processes with jets faking isolated leptons. The search for resonant production is performed by examining the reconstructed $t\bar{t}$ invariant mass distribution.

This analysis has previously been performed in Run I by DØ [6] and CDF [7]. For Run II, preliminary conference results exist for DØ [8] and CDF [9, 10] finding no evidence for a $t\bar{t}$ resonance.

In these studies a topcolor model was used as a reference to quote mass limits. In this model [5] a large top quark mass can be generated through the formation of a dynamical $t\bar{t}$ condensate, X, which is formed by a new strong gauge force coupling preferentially to the third generation of fermions. In one particular model, topcolor-assisted technicolor [11], X couples weakly and symmetrically to the first and second generations and strongly only to the third generations of quarks and has no couplings to leptons. This model results in a predicted cross section for $t\bar{t}$ production larger than the standard model (SM) prediction.

Limits obtained on $\sigma_X \times B(X \to t\bar{t})$ were used to quote a limit on the mass of such a topcolor Z'. The most recent results yield $M_{Z'} > 680$ GeV for the DØ analysis [8] and $M_{Z'} > 725$ GeV for the CDF analysis [9, 10], both for a resonance with $\Gamma_X = 0.012 M_X$.

II. DØ DETECTOR

The Run II DØ detector contains the following main components: the central tracking system, the liquid-argon/uranium calorimeter, and the muon spectrometer.

The central tracking system includes a silicon microstrip tracker (SMT) and a central fiber tracker (CFT), both located within a 2 T superconducting solenoid magnet. The SMT is designed to provide efficient tracking and vertexing capability at pseudorapidities of $|\eta| < 3$ [12]. The system has a six-barrel longitudinal structure, each with a set of four layers arranged axially around the beampipe, and interspersed with 16 radial disks. A typical pitch of 50-80 μm of the SMT strips allows a precision determination of the three-dimensional track impact parameter with respect to the primary vertex which is the key component of the b-tagging algorithm used in this analysis. The CFT has eight coaxial barrels, each supporting two doublets of overlapping scintillating fibers of 0.835 mm diameter, one doublet being parallel to the collision axis, and the other alternating by $\pm 3^o$ relative to the axis [13].

The calorimeter is divided into a central section (CC) providing coverage out to $|\eta| \approx 1$, and two end calorimeters (EC) extending coverage to $|\eta| \approx 4$ all housed in separate cryostats. Scintillators placed between the CC and EC provide sampling of showers at $1.1 < |\eta| < 1.4$ [14].

The muon system, covering pseudorapidities of $|\eta| < 2$, is located beyond the calorimetry, and consists of three layers of tracking detectors and scintillating trigger counters. Moving radially outwards, the first layer is placed before the 1.8 T solid iron toroidal magnets, and the two following layers are located after the magnets [15].

III. EVENT SELECTION

The event selection in the e+jets and μ+jets channel requires either an isolated electron with $p_T > 20\,\mathrm{GeV}$ and $|\eta| < 1.1$, or an isolated muon with $p_T > 20\,\mathrm{GeV}$ and $|\eta| < 2.0$. No additional isolated leptons with $p_T > 15\,\mathrm{GeV}$

are allowed in the event. More details on the lepton identification as well as trigger requirements are reported elsewhere [16, 17]. We require $\not\!\!E_T$ to exceed 20 GeV (25 GeV) for the e+jets (μ+jets) channel and to not be collinear with the lepton direction in the transverse plane. Jets are defined using a cone algorithm with radius $\Delta\mathcal{R} = 0.5$ [18], where $\Delta R = \sqrt{\Delta\phi^2 + \Delta\eta^2}$. The selected events must contain four or more jets with $p_T > 20$ GeV and rapidity $|y| < 2.5$ [12]. One of the jets is required to have $p_T > 40$ GeV. In the muon+jets channel, events with a mismeasured muon momentum are rejected by requiring $\Delta\phi(\mu, \not\!\!E_T) > 2.1 - 0.035\,\not\!\!E_T$, where $\Delta\phi(\mu, \not\!\!E_T)$ denotes the azimuthal angle between the muon and $\not\!\!E_T$ directions.

In order to improve the signal-to-background ratio, at least one jet is required to be identified as a b-jet. The tagging algorithm uses a neural network to combine track impact parameter [19] information with decay length [20] properties of any reconstructed secondary vertex within the cone of a given jet. The output variable, NN_B, is near one for b-jets and near zero for light jets [21].

IV. MONTE CARLO SIMULATION

Monte Carlo (MC) samples corresponding to resonant $t\bar{t}$ production are generated with PYTHIA [22], using the CTEQ6L1 [23] parton distribution functions, for ten different choices of the resonance mass M_X: 350, 400, 450, 500, 550, 600, 650 750, 850 GeV and 1 TeV. In all cases, the width of the resonance is set to $\Gamma_X = 0.012 M_X$. This qualifies X as a narrow resonance since its width is smaller than the expected mass resolution of the DØ detector (about $0.04 M_X$ in Run I). This particular choice of Γ_X was made in order to compare the results to those quoted in Refs. [6, 7]. The generated resonance is forced to decay into $t\bar{t}$ and only the events with one W boson decaying leptonically (including $W \to \tau\nu$) and the other W boson decaying hadronically are selected for further processing through the detector simulation and reconstruction chain.

All MC samples for the background processes, $t\bar{t}$ and W+jets, are generated using ALPGEN [24] for the hard interaction. For subsequent generation of parton shower, hadronization and hadron decays PYTHIA 6.323 is used. The set of parton distribution functions used in both generators is CTEQ6L1 [23]. The W+jets samples have been generated with ALPGEN [24] using PYTHIA to shower the generated partons and following the MLM prescription [25] for matching the parton shower to the matrix element.

In the generation of both resonant and non-resonant $t\bar{t}$ production, a top quark mass $m_t = 175$ GeV is assumed. All generated events have been processed through the full GEANT-based [26] DØ detector simulation and the same reconstruction program used for data.

V. RECONSTRUCTION OF THE $t\bar{t}$ INVARIANT MASS DISTRIBUTION

The $t\bar{t}$ invariant mass is reconstructed directly from the four leading jet four-momenta and the lepton momentum. The required neutrino momentum is obtained from the transverse missing energy, $\not\!\!E_T$, and by solving $M_W^2 = (p^l + p^\nu)^2$ for the z-component of the neutrino momentum. In case of two solutions the one with the lower absulute p_z^ν is taken; if no solution exists, p_z^ν is set to 0. This method was shown to give better sensitivity for high mass resonances than a previously applied constrained kinematic fit technique [27], while only slightly reducing the sensitivity for lower resonance masses.

The expected $t\bar{t}$ invariant mass distributions for three different resonance masses are compared to the Standard Model expectation in Figure 1.

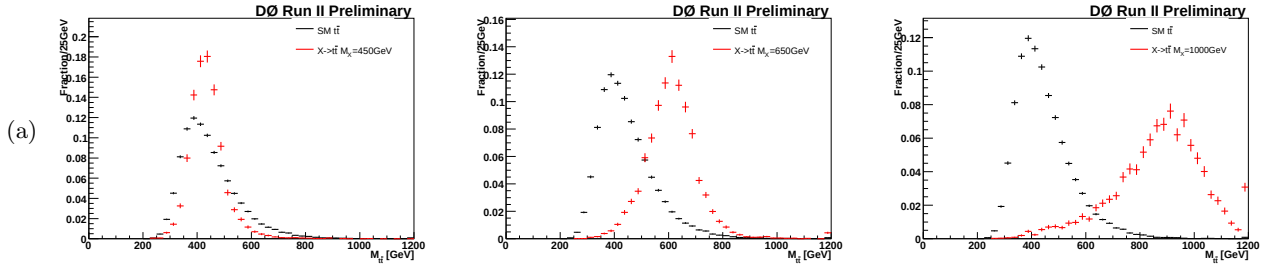

$M_X = 450$ GeV $\quad$ $M_X = 650$ GeV $\quad$ $M_X = 1$ TeV

FIG. 1: Shape comparison of expected $t\bar{t}$ invariant mass distribution for resonant production from narrow-width resonances of mass $M_X = 450$, 650 GeV and $M_X = 1$ TeV (red) compared to Standard Model production (black).

VI. BACKGROUND ESTIMATION

Before b-tagging, the main background is W+jets, where the W boson decays leptonically. In most cases, the jets accompanying the W boson originate from light (u, d, s) quarks and gluons, and only $\sim 20\%$ of events with ≥ 4 jets in the final state contain at least one jet resulting from the fragmentation of a heavy (b or c) quark. The next largest contribution is SM $t\bar{t}$ production, followed by multijet production, with one of the jets misidentified as a lepton and accompanied by large $\not\!\!E_T$ resulting from mismeasurements of jet energies. A significantly smaller contribution results from electroweak production of a single top quark. Backgrounds resulting from diboson (WW,WZ and ZZ) as well as Z/γ^* production are estimated to be small. After b-tagging, only $\sim 4\%$ of W+jets but $\sim 60\%$ of $t\bar{t}$ events remain, which makes SM $t\bar{t}$ production the dominant background in this analysis.

The SM $t\bar{t}$ background is estimated by making use of the MC simulation, both to predict the total acceptance as well as the shape of the $t\bar{t}$ invariant mass distribution. In the evaluation of the acceptance, event trigger, reconstruction and tagging efficiencies measured in data are taken into account. The tagging probability for each event is estimated by applying the tagging rates measured in data (tag rate functions or TRFs) to each jet in the simulation, taking into consideration its flavor, p_T, and η. Finally, the expected yield is normalized to the SM theoretical prediction for the $t\bar{t}$ production cross section: $\sigma_{t\bar{t}} = 6.77 \pm 0.60$ pb for $m_t = 175\,\text{GeV}$ [28].

The W+jets background is estimated from a combination of data and MC information. The expected number of W+jets events in the tagged sample is computed as the product of the estimated number of W+jets before tagging and the expected event tagging probability. The former is obtained from the estimated number of events with real leptons in data, computed using the method described in Ref. [16] (Matrix Method) and after subtraction of the expected contributions from SM $t\bar{t}$ and single top production. The tagging probability is obtained by combining the W+jets flavor fractions estimated from MC with the event tagging probability, estimated from tagging rates measured in data, for each flavor configuration. The shape of the reconstructed $t\bar{t}$ invariant mass distribution is obtained from the MC simulation.

The multijet background is completely determined from data. The total number of expected events is estimated by applying the Matrix Method on the tagged sample. This method allows for the determination of the total normalization for this background source but, due to the limited available statistics, not the shape of the reconstructed $t\bar{t}$ invariant mass distribution, which is derived from a larger sample of events with the lepton failing the strict isolation requirements and without requiring b-tagging. The kinematic biases resulting from the b-tagging requirement are mimicked by applying per-jet tag rate functions measured in data.

A summary of the prediction for the different background contributions in the combined ℓ+jets channels, along with the observed number of events in data, is given in Table I.

Yield table	
Contribution	>= 4 Jets
Data	197
$t\bar{t}$ ℓ+jets	148.56 ± 0.76
$t\bar{t}$ ll	5.89 ± 0.16
ZZ	0.12 ± 0.01
WW	1.00 ± 0.04
WZ	0.31 ± 0.04
tb	1.09 ± 0.03
tbq	2.35 ± 0.05
Z+jets	3.58 ± 0.14
Wbb	9.20 ± 0.14
Wcc	5.01 ± 0.09
Wlp	3.90 ± 0.05
Multijet	6.27 ± 1.76
sum_bkg	187..28 $\pm$ 1.30

TABLE I: Predicted and observed number of events after ≥ 1 tag with b-tag. Errors are statistical only.

VII. SYSTEMATIC UNCERTAINTIES

This analysis relies on the prediction of the overall normalization as well as the shape of the reconstructed $t\bar{t}$ invariant mass distribution for both signal and the different backgrounds. The systematic uncertainties can be classified as those affecting only normalization and those affecting both normalization and shape of the $t\bar{t}$ invariant mass distribution for one or more processes (signal or backgrounds).

The systematic uncertainties affecting only the normalization include, e.g., the experimental uncertainties on the MC-to-data correction factors and the theoretical uncertainty on the SM prediction for $\sigma_{t\bar{t}}(m_t = 175\,\text{GeV})$ (9%) [28] and the uncertainty on the integrated luminosity (6.1%) [29].

The systematic uncertainties affecting the shape of the $t\bar{t}$ invariant mass distribution in addition to the normalization have been studied both on signal and background samples. These include, e.g., uncertainties on the jet energy calibration, jet reconstruction efficiency and b-tagging parameterizations for b, c and light jets. The top quark mass is known with limited accuracy and thus contributes a systematic uncertainty: it affects the normalization due to the mass-dependence of $\sigma_{t\bar{t}}$ and modifies the invariant mass distribution expected in the Standard Model. To study the resulting systematic effect, $t\bar{t}$ MC samples with $m_t = 165\,\text{GeV}$ and $m_t = 185\,\text{GeV}$, normalized to the corresponding theoretical prediction ($\sigma_{t\bar{t}} = 9.28$ pb and 4.98 pb, respectively), have been used. This wide variation was treated as a 2σ variation and the resulting effect was scaled correspondingly. The difference in the total acceptance due to top quark mass variation has also been included in the systematic uncertainty.

The systematic uncertainties associated with the estimate of the fractions for the different flavor components of the W+jets background have been taken into account as well as uncertainties from jet taggability, parametrisation of b-fragmentation and the efficiencies used in the Matrix Method that determines the amount of W+jets and multijet background (denoted as multijet lepton fake rate).

Table II gives a summary of the relative systematic uncertainties on the total SM background expectation for the combined ℓ+jets channels. The effect of the different systematic uncertainties on the shape of the $t\bar{t}$ invariant mass distribution can not be inferred from this table, but is included in the analysis.

source	rel. sys. uncertainty (%) Standard Model processes (%)		Resonance $M_X = 750\,\text{GeV}$	
	σ^+	σ^-	σ^+	σ^-
Jet energy scale	+5.87	−6.08	+5.11	-5.44
Jet energy resolution	+0.00	−0.06	0.00	-0.91
Jet identification	–	−2.09	-	-2.12
$\sigma_{t\bar{t}}(m_t = 175\,\text{GeV})$	+6.24	−6.24	-	-
b-tag TRFs	+3.63	−3.79	4.28	-4.40
c-tag TRFs	+0.34	−0.34	+0.0	-0.08
light tag TRFs	+0.22	−0.22	-0.12	-0.17
Taggability	+1.31	−1.33	+1.45	+1.45
Heavy flavor scale factor for W+jets	+0.77	−0.84	-0.95	+1.12
b fragmentation reweighting	+0.92	–	+0.91	–
Multijet lepton fake rate	+0.05	−0.05	-	-
Luminosity	+4.47	−4.48	+6.15	-6.10
Top mass variation	+8.05	−6.60	-	-

TABLE II: Summary of the relative systematic change on the overall normalization of the Standard Model background and for an resonance mass of $M_X = 750\,\text{GeV}$.

VIII. RESULT

After all selection cuts, 95 events remain in the e+jets channel and 102 events in the μ+jets channel. Figure 2 shows the $t\bar{t}$ invariant mass for the combined ℓ+jets channels for the selected events in data and for the SM background predictions (see Sect. VI). The $t\bar{t}$ invariant mass distribution is used to perform a binned likelihood fit of the signal and background expectations compared to data.

Assuming there is no resonance signal, a Bayesian approach is used to calculate 95% C.L. upper limits on $\sigma_X \times B(X \to t\bar{t})$ for each hypothesized M_X discussed in Sect. IV. A Poisson distribution is assumed for the number of observed events in each bin, as well as flat Bayesian prior probabilities for $\sigma_X \times B(X \to t\bar{t})$. Systematic uncertainties on the signal acceptance and background yields are implemented via a convolution procedure of a multivariate Gaussian distribution implementing a full covariance matrix including correlations [30].

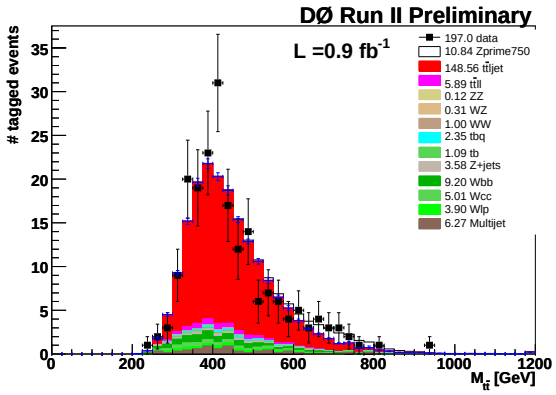

FIG. 2: The resulting $t\bar{t}$ invariant mass distribution for the combined ℓ+jets channels. The error bars drawn on top of the SM background indicate the statistical uncertainty. Superimposed as white area is the expected signal for a topcolor-assisted technicolor Z' with $M_{Z'} = 750\,\text{GeV}$.

M_X [GeV]	exp. limit [pb]	obs. limit [pb]
350	1.83	2.44
400	1.92	2.93
450	1.81	2.32
500	1.56	1.16
550	1.22	0.83
600	0.90	0.81
650	0.70	0.92
750	0.49	0.79
850	0.42	0.62
1000	0.36	0.45

TABLE III: Expected and observed limits for $\sigma_X \times B(X \to t\bar{t})$ at the 95% C.L. with systematic uncertainties taken into account.

The expected and observed 95% C.L. upper limits on $\sigma_X \times B(X \to t\bar{t})$ as a function of M_X are summarized in Table III and displayed in Fig. 3. This figure also includes the predicted $\sigma_X \times B(X \to t\bar{t})$ for a leptophobic Z' boson with $\Gamma_{Z'} = 0.012 M_{Z'}$ computed using CTEQ6L1 parton distribution function which, combined with the experimental limits, excludes $M_{Z'} < 680\,\text{GeV}$ at 95% C.L. The expected cross-section limits as a function of M_X have improved with respect to a previous analysis performed with $370\,\text{pb}^{-1}$ [8] which gave an expected limit to the Z' mass of 650 GeV, compared to the current expected limit on the Z' mass of 740 GeV.

IX. CONCLUSION

A search for a narrow-width heavy resonance decaying to $t\bar{t}$ in the ℓ+jets final states has been performed using data corresponding to an integrated luminosity of about $0.9\,\text{fb}^{-1}$, collected with the DØ detector during Run II of the Tevatron collider. By analyzing the reconstructed $t\bar{t}$ invariant mass distribution and using a Bayesian method, model independent upper limits on $\sigma_X \times B(X \to t\bar{t})$ have been obtained for different hypothesized masses of a narrow-width heavy resonance decaying into $t\bar{t}$. Within a topcolor-assisted technicolor model, the existence of a leptophobic Z' boson with $M_{Z'} < 680\,\text{GeV}$ and width $\Gamma_{Z'} = 0.012 M_{Z'}$ can be excluded at 95% C.L..

Acknowledgments

We thank the staffs at Fermilab and collaborating institutions, and acknowledge support from the DOE and NSF (USA); CEA and CNRS/IN2P3 (France); FASI, Rosatom and RFBR (Russia); CAPES, CNPq, FAPERJ, FAPESP and FUNDUNESP (Brazil); DAE and DST (India); Colciencias (Colombia); CONACyT (Mexico); KRF (Korea); CONICET and UBACyT (Argentina); FOM (The Netherlands); PPARC (United Kingdom); MSMT (Czech

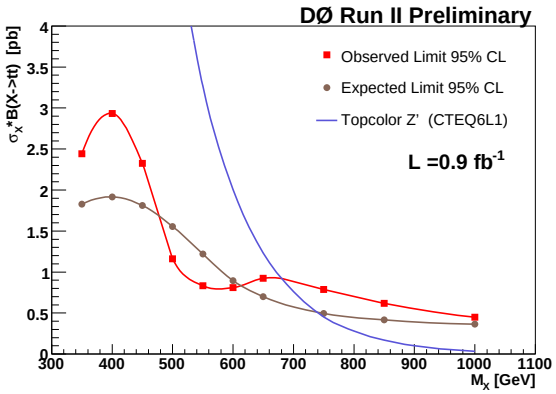

FIG. 3: Expected and observed 95% C.L. upper limits on $\sigma_X \times B(X \to t\bar{t})$ compared with the predicted topcolor-assisted technicolor cross section for a Z' boson with a width of $\Gamma_{Z'} = 0.012 M_{Z'}$ as a function of resonance mass M_X.

Republic); CRC Program, CFI, NSERC and WestGrid Project (Canada); BMBF and DFG (Germany); SFI (Ireland); Research Corporation, Alexander von Humboldt Foundation, and the Marie Curie Program.

[1] A. Leike, Phys. Rept. **317**, 143 (1999) [arXiv:hep-ph/9805494].
[2] B. Lillie, L. Randall and L. T. Wang, arXiv:hep-ph/0701166.
[3] T. G. Rizzo, Phys. Rev. D **61**, 055005 (2000) [arXiv:hep-ph/9909232].
[4] L. M. Sehgal and M. Wanninger, Phys. Lett. B **200**, 211 (1988).
[5] C. T. Hill and S. Parke, Phys. Rev. D **49**, 4454 (1994).
[6] DØ Collaboration, V.M. Abazov *et al.*, Phys. Rev. Lett. **92**, 221801 (2004).
[7] CDF Collaboration, T. Affolder *et al.*, Phys. Rev. Lett. **85**, 2062 (2000).
[8] T. DØ Collaboration, *Search for a $t\bar{t}$ Resonance in $p\bar{p}$ Collisions at $\sqrt{s} = 1.96$ TeV in the Lepton+Jets Final State* , 2005. DØ Note 4880-CONF.
[9] T. C. Collaboration, *Search for resonant $t\bar{t}$ production in $p\bar{p}$ Collisions at $\sqrt{s} = 1.96$ TeV*, 2006. CDF Note 8087.
[10] T. C. Collaboration, *Limit on resonant $t\bar{t}$ production in $p\bar{p}$ Collisions at $\sqrt{s} = 1.96$ TeV*, 2006. CDF Note 8675.
[11] R. M. Harris, C. T. Hill and S. Parke, hep-ph/9911288 (1999).
[12] Rapidity y and pseudorapidity η are defined as functions of the polar angle θ and parameter β as $y(\theta, \beta) \equiv \frac{1}{2} \ln [(1 + \beta \cos\theta)/(1 - \beta \cos\theta)]$ and $\eta(\theta) \equiv y(\theta, 1)$, where β is the ratio of a particle's momentum to its energy.
[13] V.M. Abazov *et al.*, (D0 Collaboration),"The upgraded D0 detector, Nucl. Instrum. Methods Phys. Res. A **565**, 463 (2006). T. LeCompte and H.T. Diehl, "The CDF and DØ Upgrades for Run II", Ann. Rev. Nucl. Part. Sci. **50**, 71 (2000).
[14] DØ Collaboration, S. Abachi *et al.*, Nucl. Instrum. Methods Phys. Res. A **338**, 185 (1994).
[15] V. Abazov *et al.*, FERMILAB-PUB-05-034-E (2005).
[16] DØ Collaboration, V. Abazov *et al.*, hep-ex/0504043.
[17] DØ Collaboration, V. Abazov *et al.*, hep-ex/0504058.
[18] We use the iterative, seed-based cone algorithm including midpoints, as described on p. 47 in G. C. Blazey *et al.* , in Proceedings of the Workshop: *"QCD and Weak Boson Physics in Run II",* edited by U. Baur, R. K. Ellis, and D. Zeppenfeld, FERMILAB-PUB-00-297 (2000).
[19] Impact parameter is defined as the distance of closest approach (d_{ca}) of the track to the primary vertex in the plane transverse to the beamline. Impact parameter significance is defined as $d_{ca}/\sigma_{d_{ca}}$, where $\sigma_{d_{ca}}$ is the uncertainty on d_{ca}.
[20] Decay length L_{xy} is defined as the distance from the primary to the secondary vertex in the plane transverse to the beamline. Decay length significance is defined as $L_{xy}/\sigma_{L_{xy}}$, where $\sigma_{L_{xy}}$ is the uncertainty on L_{xy}.
[21] T. Scanlon, Ph.D. thesis, University of London, 2006. FERMILAB-THESIS-2006-43.
[22] T. Sjostrand *et al.*, Comp. Phys. Commun. **135**, 238 (2001).
[23] H. L. Lai *et al.*, Eur. Phys. J. **C12**, 375 (2000).
[24] M.L. Mangano *et al.*, JHEP **07**, 001 (2003).
[25] S. Höche *et al.*, hep-ph/0602031.
[26] R. Brun and F. Carminati, CERN Programming Library Long Writeup **W5013** (1993).
[27] DØ Collaboration, B. Abbot *et al.*, Phys. Rev. D **58**, 052001 (1998); DØ Collaboration, S. Abachi *et al.*, Phys. Rev. Lett. **79**, 1197 (1997).
[28] R. Bonciani *et al.*, Nucl. Phys. B **529**, 424 (1998); M. Cacciari *et al.*, JHEP **0404**, 068 (2004); N. Kidonakis and R. Vogt,

Phys. Rev. D **68**, 114014 (2003); N. Kidonakis and R. Vogt, Eur. Phys. J., C **33**, 466 (2004).
[29] T. Andeen *et. al.*, FERMILAB-TM-2365-E (2006).
[30] I. Bertram *et. al.*, FERMILAB-TM-2104 (2000).